Supporting information for

2D MnO_2 nanosheets generated signal transduction with 0D carbon quantum dots: synthesis strategy, dual-mode behavior and glucose detection

Jiapei Gu [a,b], Xiangqian Li [a,b], Zhan Zhou [b*], Wanqiang Liu [c], Kai Li [a], Jinwei Gao [d], Ying Zhao [b], Qianming Wang [a*]

a. *Key Laboratory of Theoretical Chemistry of Environment, Ministry of Education, School of Chemistry & Environment, South China Normal University, Guangzhou 510006, China*

b. *College of Chemistry and Chemical Engineering, Henan Key Laboratory of Function-Oriented Porous Materials, Luoyang Normal University, Luoyang 471934, PR China*

c. *School of Chemistry and Chemical Engineering, Hunan University of Science and Technology, Xiangtan 411201, P. R. China*

d. *Guangdong Provincial Engineering Technology Research Center For Transparent Conductive Materials, South China Normal University, Guangzhou 510006, China*

*** Corresponding Author**

Tel.: 86-20-39310258, Fax: 86-20-39310187. E-mail: qmwang@scnu.edu.cn; zhouzhan@lynu.edu.cn

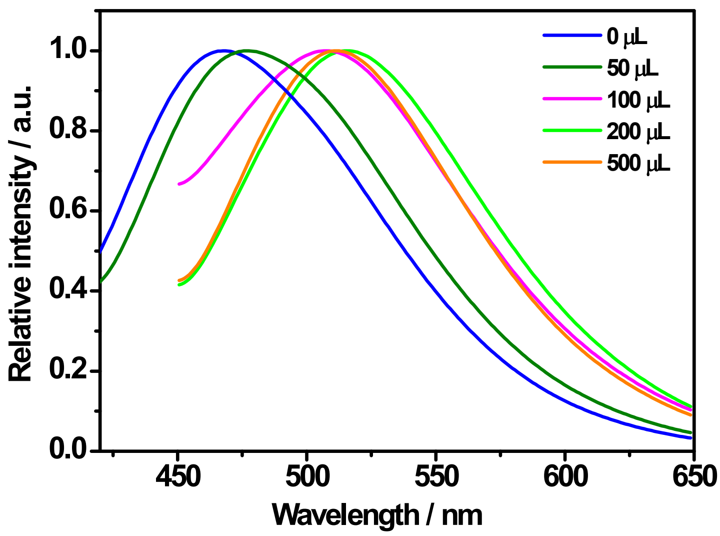

Figure S1 Emission spectra of obtained CDs (20 μg/mL) in aqueous solutions in the presence of different volume of HNO_3 (0-500 μL) (excitation wavelength at 452 nm).

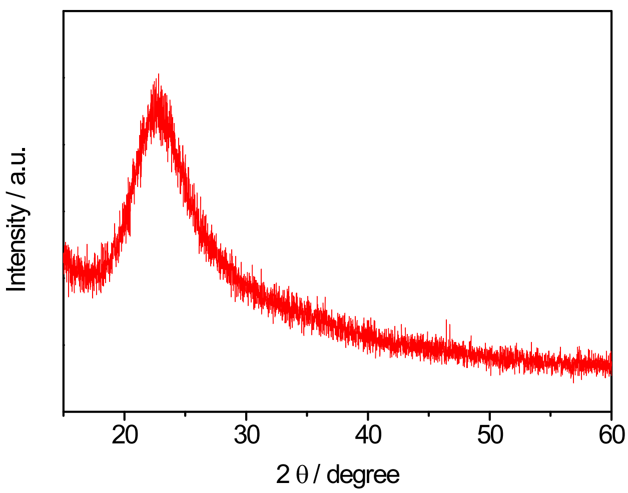

Figure S2 XRD pattern of CDs.

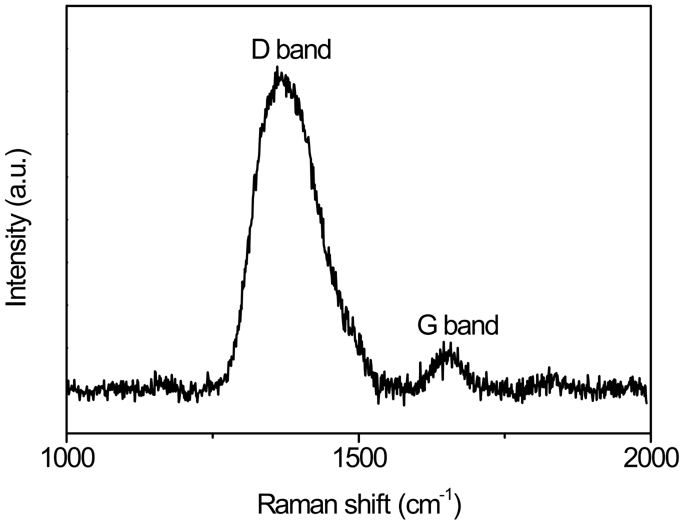

Figure S3 Raman spectrum of CDs.

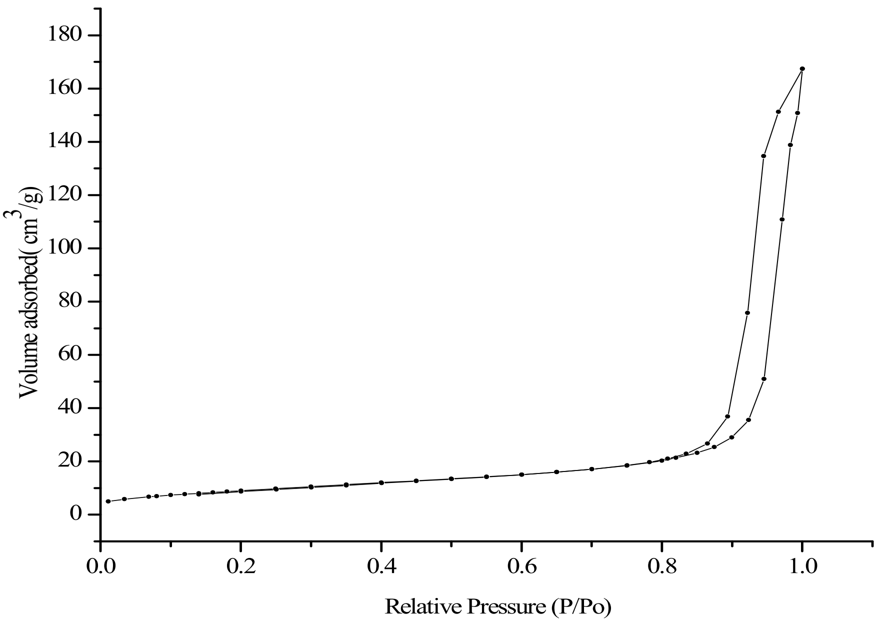

Figure S4 N_2 adsorption-desorption isotherm of CDs-MnO_2 nanocomposite.

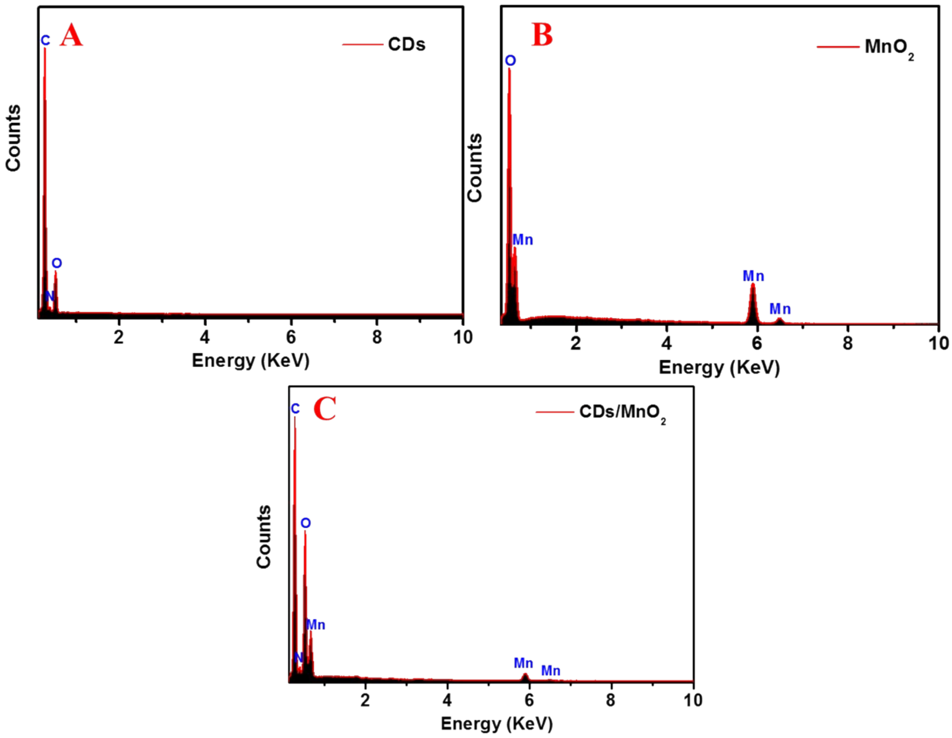

Figure S5 EDS spectra of (A) CDs, (B) MnO_2 nanosheets, (C) CDs-MnO_2 nanocomposite, respectively.

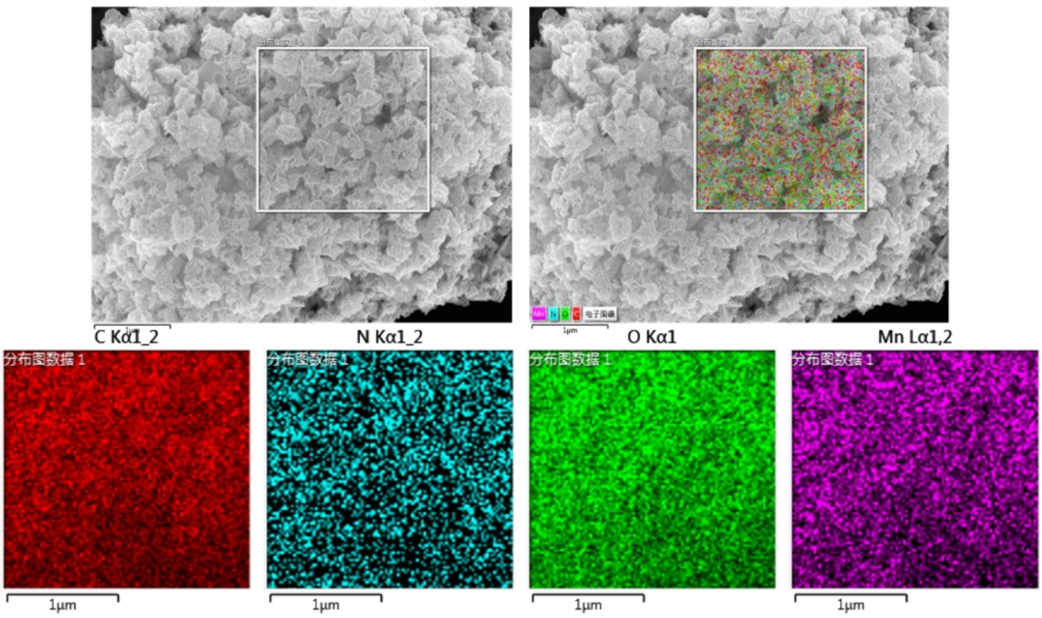

Figure S6 EDX elemental mapping of CDs-MnO_2 nanocomposite.

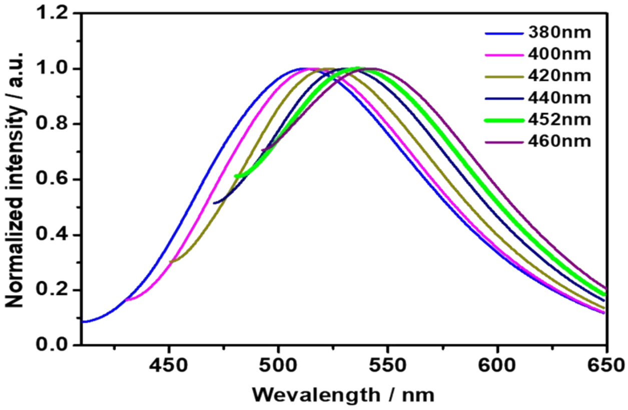

Figure S7 Normalized emission spectra of CDs (20 μg/mL) in aqueous solutions at different excitation wavelengths from 380 to 460 nm.

Table S1. Summary of the quantum yields (QY) and applications of CDs prepared by using various materials.

Materials	QY/%	Fluorescence	Application	Ref.
Bergamot	50.78	blue	Hg^{2+} and Fe^{3+} detection	1
Honey	19.8	blue	Fe^{3+} detection and cell imaging	2
Aloe	10.37	yellow	tartrazine detection	3
Lotus root	19.0	blue	Hg(II) ions detection and cell imaging	4
Bamboo leaves	7.1	blue	copper(II) ion detection	5
Prawn shells	9	blue	copper ions detection	6
Garlic	13	blue	Fe(III) ions detection and cell imaging	7
Bauhinia flower	27	blue	Fe^{3+} and adenosine triphosphate detection	8
Tulsi leaves	9.3	green	Pb^{2+} ions detection and live cell imaging	9
Gynostemma	5.7	blue	bioimaging and antioxidant	10
Peony	11.6	green	glucosedetection	This work

[1] J. Yu, N. Song, Y.K. Zhang, S.X. Zhong, A.Jun. Wang, J.R. Chen, Green preparation of carbon dots by Jinhua bergamot for sensitiveand selective fluorescent detection of $Hg^{2+}$and Fe^{3+}, Sensor. Actuat. B-Chem. 214 (2015) 29-35.

[2] X.M. Yang, Y. Zhuo , S.S. Zhu, Y.W. Luo, Y.J. Feng, Y. Dou, Novel and green synthesis of high-fluorescent carbon dots originated from honey for sensing and imaging, Biosens. Bioelectron. 60 (2014) 292-298.

[3] H. Xu, X.P. Yang, G. Li, C. Zhao, and X.J. Liao, Green synthesisoffluorescent carbon dots for selective detection of tartrazine in food samples, J. Agric. Food Chem. 63 (2015) 6707-6714.

[4] D. Gu, S.M. Shang, Q. Yu, J. Shen, Green synthesis of nitrogen-doped carbon dots from lotus root for Hg(II) ions detection and cell imaging, Appl. Surf. Sci. 390 (2016) 38-42.

[5] Y.S. Liu, Y.N. Zhao, Y.Y. Zhang, One-step green synthesized fluorescent carbon nanodots frombamboo leaves for copper(II) ion detection, Sensor. Actuat. B-**C**hem. 196 (2014) 647-652.

[6] G. Gedda, C.Y. Lee, Y.C. Lin, H.F. Wu,Green synthesis of carbon dots from prawn shells for highly selectiveand sensitive detection of copper ions, Sensor. Actuat. B-Chem. 224 (2016) 396-403.

[7] Y.F. Chen, Y.Y. Wu, B. Weng, B. Wang, C.M. Li, Facile synthesis of nitrogen and sulfur co-doped carbon dots and application for Fe(III) ions detection and cell imaging, Sensor. Actuat. B-Chem. 23 (2016) 689–696.

[8] Q.T. Huang, Q. Li, Y.F. Chen, L.L. Tong, X.F. Lin, J.J. Zhu, Q.X. Tong, High quantum yield nitrogen-doped carbon dots: green synthesis and application as“off-on” fluorescent sensors for the determination of Fe^{3+} andadenosine triphosphate in biological samples, Sensor. Actuat. B-Chem. 276 (2018) 82-88.

[9] A. Kumar, A.R. Chowdhuri, D. Laha, T.K. Mahto,P. Karmakar, S.K. Sahu, Green synthesis of carbon dots from ocimum sanctum for effective fluorescent sensing of Pb^{2+} ions and live cell imaging, Sensor. Actuat. B-Chem. 242 (2017) 679-686.

[10] X.J. Wei, L. Li, J.L. Liu, L.D.Yu, H.B. Li, F. Cheng, X.T. Yi, J.M. He,B.S. Li, Green synthesis of fluorescent carbon dots from gynostemma for bioimaging and antioxidant in zebrafish, ACS Appl. Mater. Interfaces 2019, 11, 9832-9840.

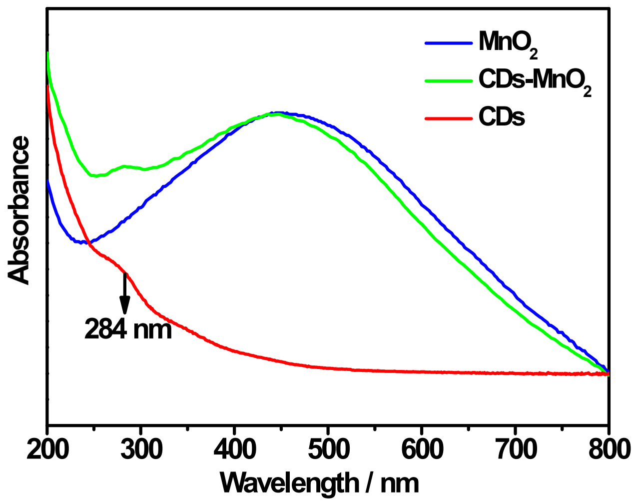

Figure S8 UV-vis absorption spectra of CDs (20 μg/mL, red line), MnO_2 (750 μM, blue line) and CDs-MnO_2 (20 μg/mL CDs + 750 μM MnO_2, green line) in aqueous solution.

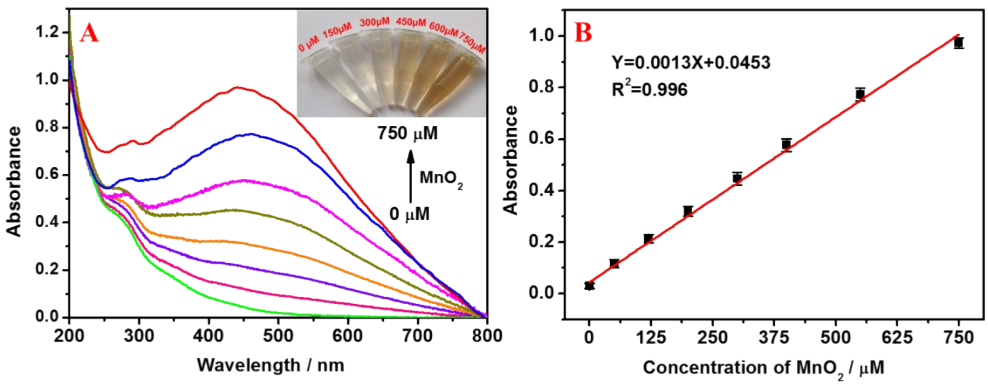

Figure S9 UV-visible spectra of CDs (20 μg mL^{-1}) in aqueous solutions with the addition of various concentrations of MnO_2 nanosheets from 0 to 750 μM. (B) Linear calibration curve between the absorbance of CDs aqueous solution and the concentration of MnO_2 nanosheets. The error bars represent the standard deviation of three replicate measurements.

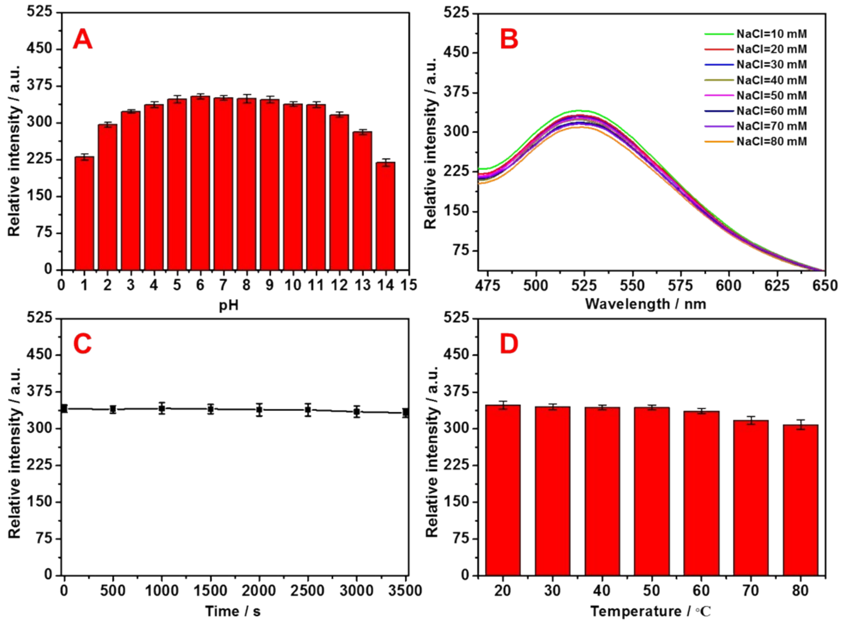

Figure S10 Fluorescent intensity of CDs-MnO_2 nanocomposite (20 μg/mL CDs + 300 μM MnO_2) in aqueous solutions at various pH values (A);different concentrations of NaCl range from 10-80 mM (B); ultraviolet irradiation from 0 to 3600 s (C); different temperature ranging from 20 to 80℃(D). (λ_{ex} = 452 nm, λ_{em} = 523 nm). The error bars represent the standard deviation of three replicate measurements.

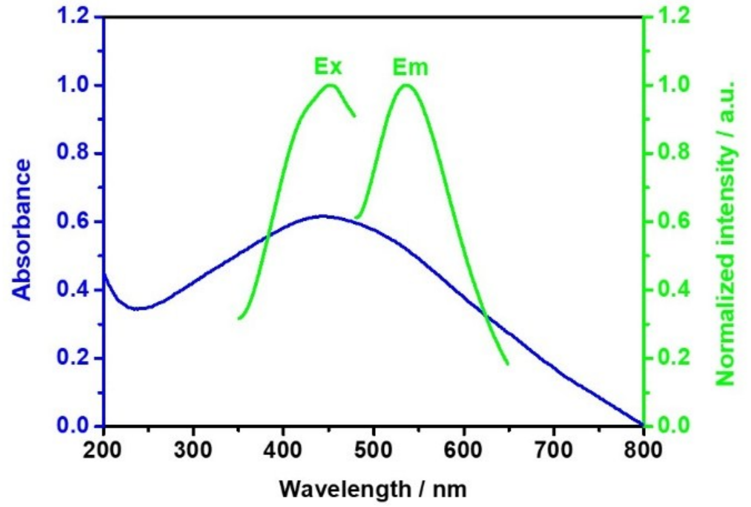

Figure S11 UV-vis absorption of MnO_2 nanosheets (750 μM) (blue line) and optimal fluorescence excitation and emission spectra of the CDs (20 μg/mL) in aqueous solutions (green line) (λ_{ex} = 452 nm, λ_{em} = 523 nm).

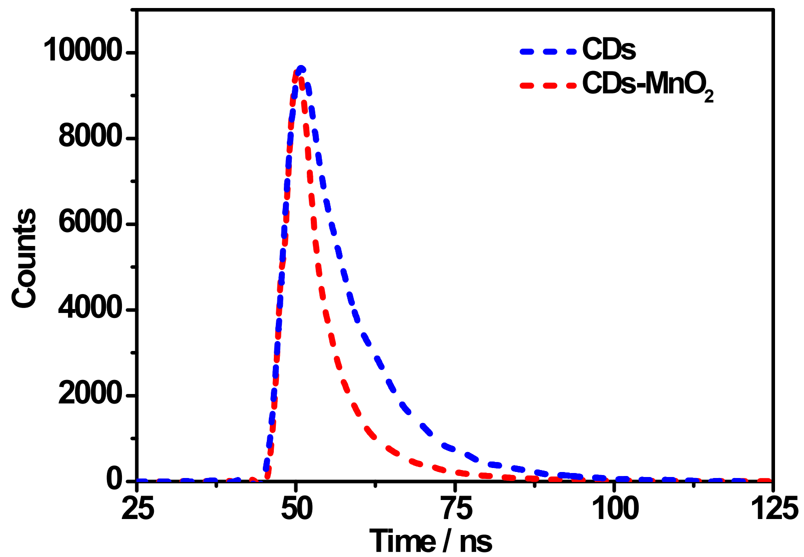

Figure S12 Lifetime measurements of CDs (blue line) and CDs-MnO_2 (red line) (λ_{ex} = 452 nm, λ_{em} = 523 nm).

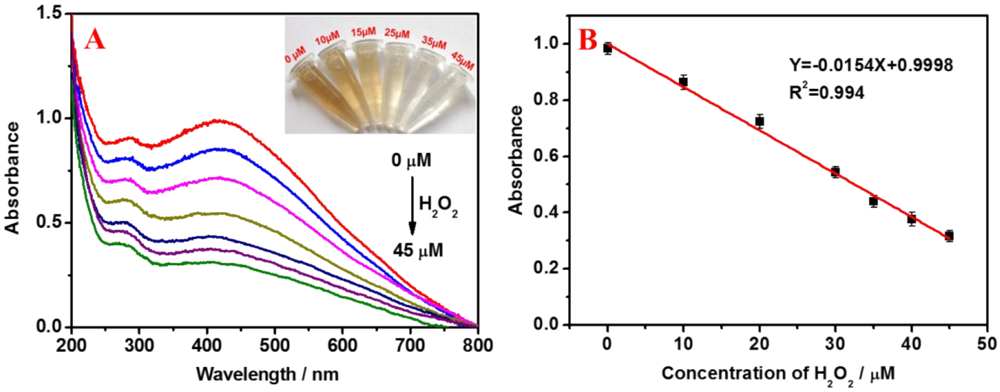

Figure S13 UV-visible spectra of CDs-MnO_2 nanocomposite (20 μg/mL CDs + 300 μM MnO_2) in aqueous solutions with the addition of various concentrations of H_2O_2 from 0 to 45 μM. (B) Linear calibration curve between the absorbance of CDs-MnO_2 nanocomposite and the concentration of H_2O_2. The error bars represent the standard deviation of three replicate measurements.

Table S2 Comparison of different materials for the determination of glucose

Materials	Detection mode	Detection limit	Ref.
Lanthanum incorporated MCM-41	Colorimetric	37.5 μM	1
$CePO_4$:Tb/Au	Fluorometric	5.25 μM	2
Cu/Ni based MOF	Electrochemical	0.06 μM	3
Bodipy derivative	Fluorometric	2.19 μM	4
MOF nanosheet	Fluorometric	1.3 μM	5
Peony-derived carbon dots-MnO_2	Fluorometric	0.18 μM	This work

[1] S. Jabariyan, M. A. Zanjanchi, M. Arvand, S. Sohrabnezhad, Colorimetric detection of glucose using lanthanum-incorporated MCM-41, Spectrochim. Acta A 203 (2018) 294-300.

[2] G.W. Yan, Y. Zhang, W.H. Di, W.P. Qin, Synthesis of luminescent $CePO_4$:Tb/Au composite for glucose detection, Dyes and Pigments 159 (2018) 28-34.

[3] X.L. Xiao, S.H. Peng, C. Wang, D. Cheng, N. Li, Y.L. Dong, Q.H. Li, D.G. Wei, P. Liu, Z.Z. Xie, D.Y. Qu, X. Li, Metal/metal oxide@carbon composites derived from bimetallic Cu/Ni-based MOF and their electrocatalytic performance for glucose sensing, J. Electroanal. Chem. 841 (2019) 94-100.

[4] B. Unal, M. Akarsu, R. Kilincarslan, D.O. Demirkol, S. Timur, B. Cetinkaya, Novel fluorescence assay using μ-wells coated by BODIPY dye as an enzymatic sensing platform, Measurement 135 (2019) 145-150.

[5] D. Ning, Q. Liu, Q. Wang, X.M. Du, W.J. Ruan, Y. Li, Luminescent MOF nanosheets for enzyme assisted detection of H_2O_2 and glucose and activity assay of glucose oxidase, Sensors

Actuat. B-Chem. 282 (2019) 443-448.

Table S3 Determination of glucose in human serum samples.

Sample	Spiked (μM)	Measured (μM)	Recovery (%)	RSD (%)
1	0	38.05±0.1	/	/
2	50.0	85.6±0.14	95.1	2.62
3	100.0	143.9±0.17	105.8	4.08
4	150.0	187.3±0.12	99.5	2.19